Theory of Pump-Probe Experiments of Metallic Metamaterials Coupled to a Gain Medium

Zhixiang Huang,[1,2] Th. Koschny,[1] and C. M. Soukoulis[1,3]

[1]*Ames Laboratory and Department of Physics and Astronomy, Iowa State University, Ames, Iowa 50011, USA*
[2]*Key Laboratory of Intelligent Computing and Signal Processing, Anhui University, Hefei 230039, China*
[3]*Institute of Electronic Structure and Laser, FORTH, 71110 Heraklion, Crete, Greece*

(Received 17 October 2011; published 4 May 2012)

We establish a new approach for pump-probe simulations of metallic metamaterials coupled to the gain materials. It is of vital importance to understand the mechanism of the coupling of metamaterials with the gain medium. Using a four-level gain system, we have studied light amplification of arrays of metallic split-ring resonators with a gain layer underneath. We find that the differential transmittance $\Delta T/T$ can be negative for split-ring resonators on the top of the gain substrate, which is not expected, and $\Delta T/T$ is positive for the gain substrate alone. These simulations agree with pump-probe experiments and can help to design new experiments to compensate for the losses of metamaterials.

DOI: 10.1103/PhysRevLett.108.187402 PACS numbers: 78.67.Pt, 42.25.Bs, 78.20.Ci, 78.45.+h

The field of metamaterials has seen spectacular experimental progress in recent years [1–3]. Most metamaterials have a metal-based nanostructure and eventually suffer from conductor losses at optical frequencies, which are still orders of magnitude too large for realistic applications. In addition, metamaterial losses become an increasingly important issue when moving from multiple metal-based metamaterial layers to the bulk case [3]. Thus, the need for reducing or even compensating for the losses is a key challenge for metamaterial technologies. One promising way of overcoming the losses is based on introducing the gain material to the metamaterial. The idea of the combination of a metamaterial with an optical gain material has been investigated by several theoretical [4–7] and experimental studies [8–12]. From the experimental point of view, the realistic gain can be experimentally realized with fluorescent dyes [8], quantum dots [9,10], or semiconductor quantum wells [11,12]. All these loss compensations are mainly attributed to the coupling between metamaterial and the gain medium. Without sufficient coupling, no loss compensation can happen, nor can the transmitted signal be amplified. Therefore, it is of vital importance to understand the mechanism of the coupling between metamaterial and the gain medium. In addition, these ideas can be used in plasmonics to incorporate gain [13,14] to obtain new nanoplasmonic lasers [15,16].

In this Letter, we present a systematic theoretical model for pump-probe experiments of metallic metamaterials coupled with the gain material, described by a generic four-level atomic system. We describe the dynamical processes in metamaterials with gain; increasing the gain changes the metamaterial properties, and we need to have self-consistent calculations [4–6] to reach a steady state. The pump-probe results affect the time dependence of the population inversion and the electric field enhancement that increases the effective gain. We observe differential transmittance signals from the coupled system that are larger than for the bare gain. Furthermore, we observe a more rapid temporal decay of the differential transmittance signal for the coupled system compared to the bare gain. Both effects indicate substantial local-field-enhancement effects, which increase the effective metamaterial gain beyond the bare gain, leading to a significant reduction of the metamaterial's losses.

We model the dispersive Lorentz active medium by using a generic four-level atomic system. The population density in each level is given by N_i $(i = 0, 1, 2, 3)$. The time-dependent Maxwell's equations for isotropic media are given by $\nabla \times \mathbf{E}(r,t) = -\partial \mathbf{B}(r,t)/\partial t$ and $\nabla \times \mathbf{H}(r,t) = \partial \mathbf{D}(r,t)/\partial t$, where $\mathbf{B}(r,t) = \mu\mu_0 \mathbf{H}(r,t)$, $\mathbf{D}(r,t) = \varepsilon\varepsilon_0 \mathbf{E}(r,t) + \mathbf{P}(r,t)$, and $\mathbf{P}(r,t)$ is the dispersive electric polarization density that corresponds to the transitions between two atomic levels, N_1 and N_2. The vector $\mathbf{P}$ introduces gain in Maxwell's equations, and its time evolution can be shown to follow that of a homogeneously broadened Lorentzian oscillator driven by the coupling between the population inversion and external electric field [17]. Thus, $\mathbf{P}$ obeys the equation of motion

$$\frac{\partial^2 \mathbf{P}(r,t)}{\partial t^2} + \Gamma_a \frac{\partial \mathbf{P}(r,t)}{\partial t} + \omega_a^2 \mathbf{P}(r,t) = \sigma_a \Delta N(r,t) \mathbf{E}(r,t),$$

where Γ_a stands for the linewidth of the atomic transitions at ω_a and accounts for both the nonradiative energy decay rate as well as dephasing processes that arise from incoherently driven polarizations. In the following simulations, this value is equal to $2\pi \times 20 \times 10^{12}$ rad/s. σ_a is the coupling strength of $\mathbf{P}$ to the external electric field, and its value is taken to be 10^{-4} C^2/kg. The factor $\Delta N(r,t) = N_1(r,t) - N_2(r,t)$ is the population inversion between level 2 and level 1 that drives the polarization $\mathbf{P}$. In order to do pump-probe experiments numerically, we first pump the gain material with a short, intense Gaussian pump pulse. After a suitable time delay, we probe the structure with a weak probe pulse (see Fig. 1). In our model, an

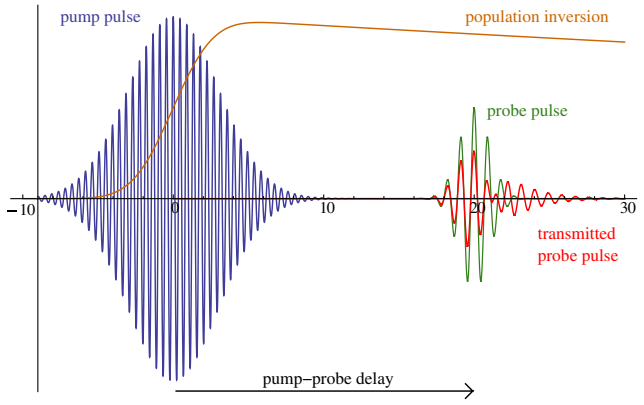

FIG. 1 (color online). Schematic illustration of pump-probe experiments.

external mechanism pumps electrons from the ground state level N_0 to the third level N_3 by using a Gaussian pumping $P_g(t)$, which is proportional to the pumping intensity in the experiments. After a short lifetime τ_{32}, electrons transfer nonradiatively into metastable second level N_2. The second level (N_2) and the first level (N_1) are called the upper and lower lasing levels, respectively. Electrons can be transferred from the upper to the lower lasing level by spontaneous and stimulated emission. At last, electrons transfer quickly and nonradiatively from the first level (N_1) to the ground state level (N_0). The lifetimes and energies of the upper and lower lasing levels are τ_{21}, E_2 and τ_{10}, E_1, respectively. The center frequency of the radiation is $\omega_a = (E_2 - E_1)/\hbar$, which is a controlled variable chosen according to the pump-probe experiments. The parameters τ_{32}, τ_{21}, and τ_{10} are chosen to be 0.05, 80, and 0.05 ps, respectively. The initial electron density $N_0(r, t = 0) = 5.0 \times 10^{23}$ m^{-3}, $N_i(r, t = 0) = 0$ m^{-3} $(i = 1, 2, 3)$. Thus, the atomic population densities obey the following rate equations:

$$\frac{\partial N_3(r,t)}{\partial t} = P_g(t)N_0(r,t) - \frac{N_3(r,t)}{\tau_{32}},$$

$$\frac{\partial N_2(r,t)}{\partial t} = \frac{N_3(r,t)}{\tau_{32}} + \frac{1}{\hbar\omega_a}\mathbf{E}(r,t)\cdot\frac{\partial \mathbf{P}(r,t)}{\partial t} - \frac{N_2(r,t)}{\tau_{12}},$$

$$\frac{\partial N_1(r,t)}{\partial t} = \frac{N_2(r,t)}{\tau_{12}} - \frac{1}{\hbar\omega_a}\mathbf{E}(r,t)\cdot\frac{\partial \mathbf{P}(r,t)}{\partial t} - \frac{N_1(r,t)}{\tau_{10}},$$

$$\frac{\partial N_0(r,t)}{\partial t} = \frac{N_1(r,t)}{\tau_{10}} - P_g(t)N_0(r,t),$$

where Gaussian pump $P_g(t) = P_0 e^{-(t-t_p/\tau_p)^2}$, with $P_0 = 3 \times 10^9$ s^{-1}, $t_p = 6$ ps [18], and $\tau_p = 0.15$ ps.

In order to solve the response of the active materials in the electromagnetic fields numerically, the finite-difference time-domain technique is utilized [19], using an approach similar to the one outlined in Ref. [20].

The object of our studies is to present pump-probe simulations on arrays of silver split-ring resonators (SRRs)

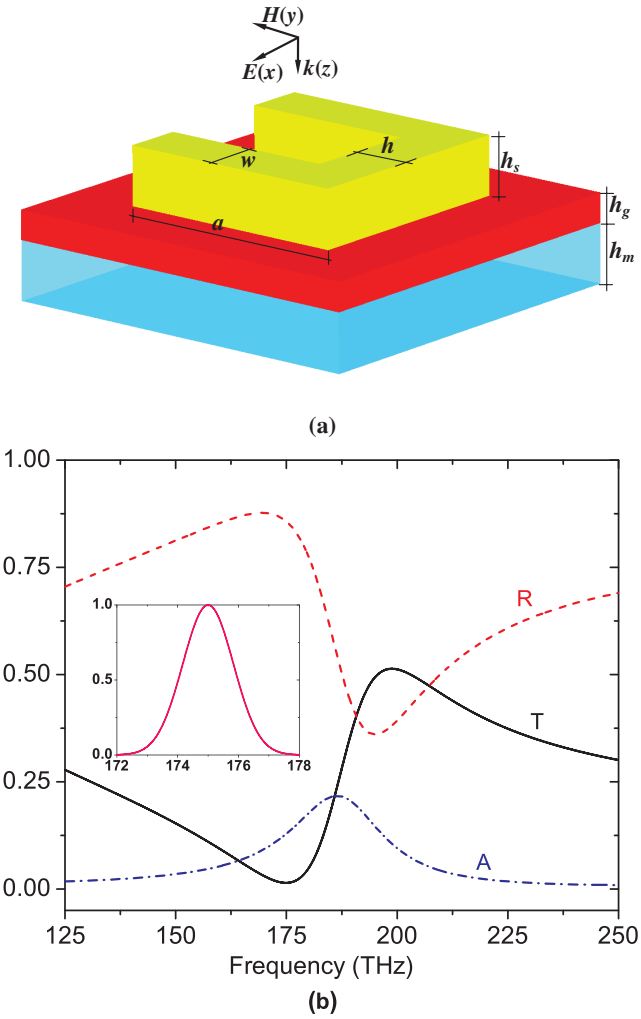

FIG. 2 (color online). (a) Schematic of the unit cell for the silver-based SRR structure (yellow) with the electric field polarization parallel to the gap. The dielectric constants ε for gain (red) and GaAs (light blue) are 9.0 and 11.0, respectively. (b) Calculated spectra for transmittance T (black), reflectance R (red), and absorptance A (blue) for the structure shown in Fig. 2(a). The inset shows the profile of the probe pulse with a center frequency of 175 THz (FWHM = 2 THz).

coupled to single quantum wells [11,12]. The structure considered is a U-shaped SRR fabricated on a gain-GaAs substrate with a square periodicity of $p = 250$ nm [see Fig. 2(a)]. The SRR is made of silver with its permittivity modeled by a Drude response: $\epsilon(\omega) = 1 - \omega_p^2/(\omega^2 + i\omega\gamma)$, with $\omega_p = 1.37 \times 10^{16}$ rad/s and $\gamma = 2.73 \times 10^{13}$ rad/s. The incident wave propagates perpendicular to the SRR plane and has the electric field polarization parallel to the gap [see Fig. 2(a)]. The corresponding geometrical parameters are $a = 150$ nm, $h_d = 40$ nm, $h_g = 20$ nm, $h_s = 30$ nm, $w = 50$ nm, and $h = 75$ nm. Figure 2(b) shows the calculated spectrum (without pump) of transmittance T, reflectance R, and absorptance A for the structure shown in Fig. 2(a). The resonant frequency is around 175 THz, and

we refer to the resonant frequency according to the dip of the transmittance. In our analysis, we first pump the active structure [see Fig. 2(a)] with a short intensive Gaussian pump pulse $P_g(t)$ [see Fig. 3, top panel]. After a suitable time delay (i.e., the pump-probe delay), we probe the structure with a weak Gaussian probe pulse with a center frequency close to the SRR resonance frequency of 175 THz. Typical examples for the spatial distribution of electric field and gain are shown in Ref. [21]. The incident electric field amplitude of the probe pulse is 10 V/m, which is well inside the linear response regime. Then, we can Fourier transform the time-dependent transmitted electric field and divide by the Fourier transform of the incident probe pulse to obtain the spectral transmittance of the system as seen by the probe pulse. Additionally, we obtain the total pulse transmittance by dividing the energy in the transmitted pulse by the energy in the incident pulse, integrated in the time domain. We define the differential transmittance $\Delta T/T$ by taking the difference of the measured total plus transmittance with pumping the active structure minus the same without pumping and dividing it by the total plus transmittance without pumping. This differential transmittance is a function of the pump-probe delay. The bottom panel in Fig. 3 gives a differential transmittance $\Delta T/T$ which is negative. This result was not expected, and we need to understand this behavior, which agrees with the experiments [11,12].

Figure 4 gives an overview of the results obtained for the case of the SRRs on resonance, i.e., $\omega_a = 2\pi \times 175 \times 10^{12}$ rad/s. Data for the structure in Fig. 2(a) (left column in Fig. 4) and for the bare gain case (right column in Fig. 4) without the SRRs on top is shown. For parallel polarization, the light does couple to the fundamental SRR resonance; for perpendicular polarization, it does not. The probe center frequency decreases from top (179 THz) to bottom (169 THz). Note that the width of the probe spectrum is 2 THz [see the inset in Fig. 2(a)]. Hence, the data have been taken with 2-THz spectral separation. Inspection of the left column shows a rather different behavior for the SRRs with gain compared to the bare gain case. While the bare gain always delivers positive $\Delta T/T$ signals below $+0.16\%$ (right column) over the whole probe spectrum, the sign and magnitude of the signals change for the case SRRs with gain. Under some conditions, $\Delta T/T$ reaches values as negative as -8.50% around $f_{\text{probe}} = 175$ THz. Additionally, we may also get positive $\Delta T/T$ at the very edges of the probe range (see the left column in Fig. 4). If we turn to the case of perpendicular polarization, no distinct change between the pump-probe results on the SRRs (not shown in Fig. 4) and the bare gain (right column in Fig. 4), neither in the magnitude nor in the dynamics of the $\Delta T/T$, can be detected.

We argue that the distinct behavior can be attributed to the strong coupling between the resonances of the SRRs and the gain medium. The negative $\Delta T/T$ are not as we expected at first glance: The pump lifts electrons from the ground state to an excited state so that the absorption of the probe pulse is reduced, leading to an increase of

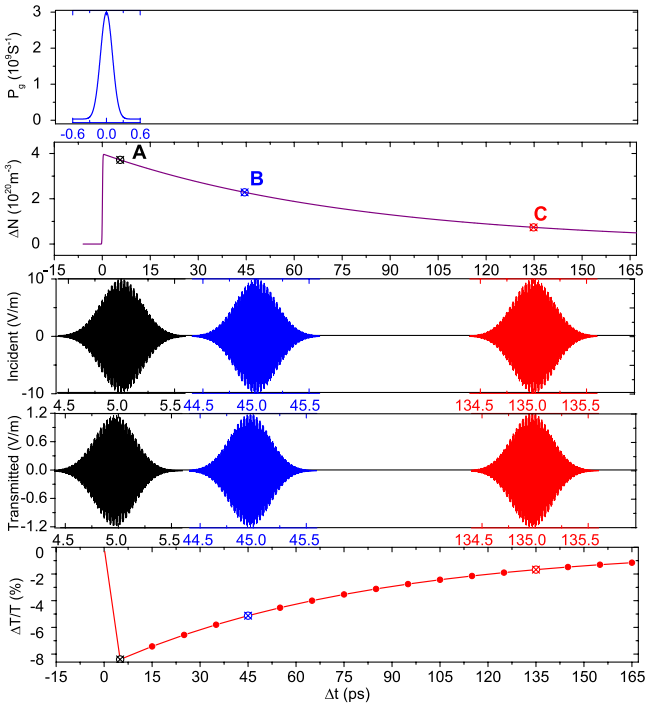

FIG. 3 (color online). Schematic of the numerical pump-probe experiments for the case on resonance. From the top to the bottom, each row corresponds to the pump pulse, population inversion, incident signal (with time delays 5, 45, and 135 ps), transmitted signal, and differential transmittance $\Delta T/T$. It should be mentioned here that the incident frequency of the probe pulse is 175 THz with a FWHM of 2 THz and is equal to the SRR resonance frequency.

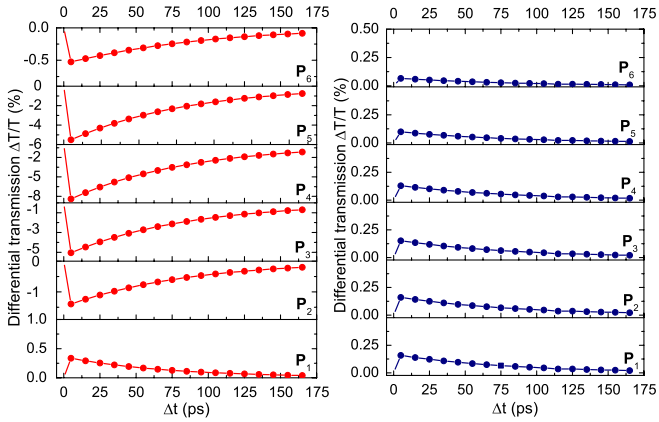

FIG. 4 (color online). Time domain numerical pump-probe experiments results for the SRR that is nearly on-resonant with the gain material. The left column corresponds to the parallel probe polarization with respect to the gap of the SRRs; the right column is the case for bare gain material, i.e., without SRRs on the top of the substrate. The width of the probe signal is 2 THz with decreasing in the probe center frequency from 179 THz for the top panel to 169 THz for the bottom panel.

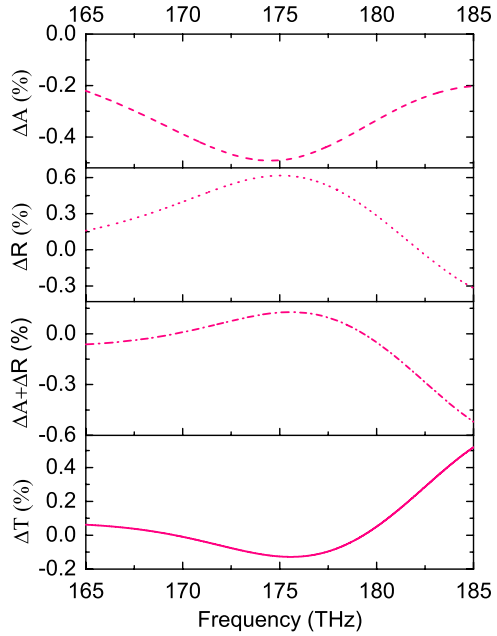

FIG. 5 (color online). Frequency domain numerical pump-probe experiments results for the on-resonance case. Simulations results for the differences in transmittance (ΔT), reflectance (ΔR), and absorptance (ΔA) versus frequency.

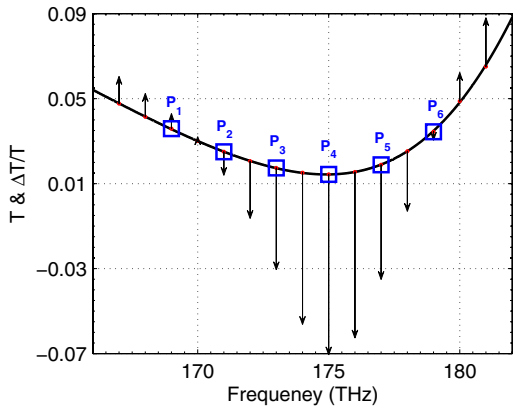

FIG. 6 (color online). The transmittance T (without pump, solid line) and the on-resonance differential transmittance $\Delta T/T$ results (vector arrow). The direction and the length of the arrow stand for the sign and the amplitude of $\Delta T/T$, respectively. The squares from $\mathbf{P}_1$ to $\mathbf{P}_6$ correspond to the frequency of probe pulse ranging from 169 to 179 THz with uniform step of 2 THz.

transmission. This is not the whole story. The reason lies in the fact that with the pump we not only affect the absorption but disturb the reflection of the structure, resulting in the mismatching of the impedance. Furthermore, we observed either an increasing or a decreasing tendency for the case of on resonance as shown in Fig. 4. All those behaviors can be explained by the competing of the weak gain resonance and the impedance mismatching between pump and without pump cases. We will explore the underlying mechanism below. Figure 5 shows the results for the difference in absorptance (ΔA), difference in reflectance (ΔR), their sum ($\Delta A + \Delta R$), and the difference in transmittance [$\Delta T = -(\Delta A + \Delta R)$] between pump ($P_0 = 3 \times 10^9$ s^{-1}) and no pump using a wide probe (FWHM = 54 THz) pulse with a fixed pump-probe delay of 5 ps. As expected, we may observe a positive differential transmittance, $\Delta T/T > 0$, when we pump the gain, $\Delta A < 0$, and if ΔR (impedance match) remains unchanged.

The results of Fig. 5 are obtained for pump-probe experiments with the probe frequency equal to the resonance frequency of the SRRs (175 THz) at a pump-probe delay of 5 ps; results for longer pump-probe delays are shown in Supplemental Material [21]. Notice that ΔR is positive, ΔA is negative, and ΔT is also negative very close to the resonance frequency. If the probe center frequency moves away from the SRR resonance frequency, the negative $\Delta T/T$ decreases in magnitude, and finally $\Delta T/T$ becomes positive. These results are shown in Fig. 6 and agree with experiments [11,12]. If we can increase the magnitude of the Gaussian pump pulse $P_g(t)$ to 5×10^{10} s^{-1} and we repeat the pump-probe experiments, $\Delta T/T \approx -100\%$ at resonance frequency, 175 THz. If we increase the pump amplitude further to 10^{11} s^{-1}, we can compensate for the losses. However, such pump intensities are unrealistic experimentally [21]. In conclusion, we have introduced a new approach for pump-probe simulations of metallic metamaterials coupled to gain materials. We study the coupling between the U-shaped SRRs and the gain material described by a four-level gain model. Using pump-probe simulations, we find a distinct behavior for the differential transmittance $\Delta T/T$ of the probe pulse with and without SRRs in both magnitude and sign (negative, unexpected, and/or positive). Our new approach has verified that the coupling between the metamaterial resonance and the gain medium is dominated by near-field interactions. Our model can be used to design new pump-probe experiments to compensate for the losses of metamaterials.

Work at Ames Laboratory was supported by the U.S. Department of Energy (Basic Energy Science, Division of Materials Sciences and Engineering) under Contract No. DE-ACD2-07CH11358. This work was partially supported by the European Community FET project PHOME (No. 213390) and by Laboratory-Directed Research and Development Program at Sandia National Laboratories. Z. H. gratefully acknowledges the support of the National Natural Science Foundation of China (No. 60931002 and No. 61101064), Distinguished Natural Science Foundation (No. 1108085J01), and Universities Natural Science Foundation of Anhui Province (No. KJ2011A002).

[1] V. M. Shalaev, Nature Photon. **1**, 41 (2007).
[2] C. M. Soukoulis, S. Linden, and M. Wegener, Science **315**, 47 (2007).
[3] C. M. Soukoulis and M. Wegener, Science **330**, 1633 (2010); Nature Photon. **5**, 523 (2011).

[4] A. Fang, Th. Koschny, and C. M. Soukoulis, Phys. Rev. B **82**, 121102(R) (2010).
[5] S. Wuestner, A. Pusch, K. L. Tsakmakidis, J. M. Hamm, and O. Hess, Phys. Rev. Lett. **105**, 127401 (2010); Phil. Trans. R. Soc. A **369**, 3525 (2011).
[6] A. Fang, Z. Huang, Th. Koschny, and C. M. Soukoulis, Opt. Express **19**, 12 688 (2011).
[7] Y. Sivan, S. Xiao, U. K. Chettiar, A. V. Kildishev, and V. M. Shalaev, Opt. Express **17**, 24 060 (2009).
[8] S. Xiao, V. P. Drachev, A. V. Kildishev, X. Ni, U. K. Chettiar, H.-K. Yuan, and V. M. Shalaev, Nature (London) **466**, 735 (2010).
[9] E. Plum, V. A. Fedotov, P. Kuo, D. P. Tsai, and N. I. Zheludev, Opt. Express **17**, 8548 (2009).
[10] K. Tanaka, E. Plum, J. Y. Ou, T. Uchino, and N. I. Zheludev, Phys. Rev. Lett. **105**, 227403 (2010).
[11] N. Meinzer, M. Ruther, S. Linden, C. M. Soukoulis, G. Khitrova, J. Hendrickson, J. D. Olitzky, H. M. Gibbs, and M. Wegener, Opt. Express **18**, 24 140 (2010).
[12] N. Meinzer, M. König, M. Ruther, S. Linden, G. Khitrova, H. M. Gibbs, K. Busch, and M. Wegener, Appl. Phys. Lett. **99**, 111104 (2011).
[13] D. J. Bergman and M. I. Stockman, Phys. Rev. Lett. **90**, 027402 (2003).
[14] M. I. Stockman, Nature Photon. **2**, 327 (2008).
[15] R. F. Oulton, V. J. Sorger, T. Zentgraf, R.-M. Ma, C. Gladden, L. Dai, G. Bartal, and X. Zhang, Nature (London) **461**, 629 (2009).
[16] M. A. Noginov, G. Zhu, A. M. Belgrave, R. Bakker, V. M. Shalaev, E. E. Narimanov, S. Stout, E. Herz, T. Suteewong, and U. Wiesner, Nature (London) **460**, 1110 (2009).
[17] A. E. Siegman, *Lasers* (University Science, Sausalito, CA, 1986), Chaps. 2, 3, 6, and 13.
[18] The pumping rate is equivalent to a pump intensity. The pump power density is equal to $\hbar\omega_a P_g N_0$, and the pump intensity $I_p = (\text{pump power})/(\text{surface area}) = \hbar\omega_a P_g N_0 (\text{volume})/(\text{surface area}) = \hbar\omega_a P_g N_0 d$, and d is the thickness of the gain layer. If we use the numbers of our simulations, $P_g = 3 \times 10^9\ \text{s}^{-1}$, $N_0 = 5 \times 10^{23}\ \text{m}^{-3}$, $\omega_a = 2\pi \times 175$ THz, and $d = 20$ nm, then $I_p = 3.5\ \text{W/mm}^2$.
[19] A. Taflove, *Computational Electrodynamics: The Finite Difference Time Domain Method* (Artech House, London, 1995), Chaps. 3, 6, and 7.
[20] A. Fang, Th. Koschny, and C. M. Soukoulis, J. Opt. **12**, 024013 (2010).
[21] See Supplemental Material at http://link.aps.org/supplemental/10.1103/PhysRevLett.108.187402 for additional details of the simulations and a discussion of overcompensation of the loss.

Supplementary material

The following two figures illustrate the spatial distribution of gain in the simulations. In Fig. S1, we have plotted the spatial distribution of the local electric field components, E_x, E_y, and E_z, with pump near the resonance of the SRR (a-c). E_x is very strong inside the SRR gap; also, the normal component E_z is reasonably strong near the ends of the open arms of the SRR. These are the locations where most of the gain originates. We plotted also the spatial distribution of the change in the electric field between pumped and unpumped transmission of the probe pulse, $\Delta E = |E_{pump}| - |E_{without\ pump}|$ where $|E| = \text{sqrt}\ (E_x^2+E_y^2+E_z^2)$, as a function of the pump-probe delay (d-e) and the strength of the pump pulse (g-h). As the pump-probe delay increases, the strength of ΔE becomes smaller; as the pumping rate increases, the amplitude of ΔE becomes bigger. This is not unexpected and simply is a consequence of the changing population inversion, i.e., the change in available local gain.

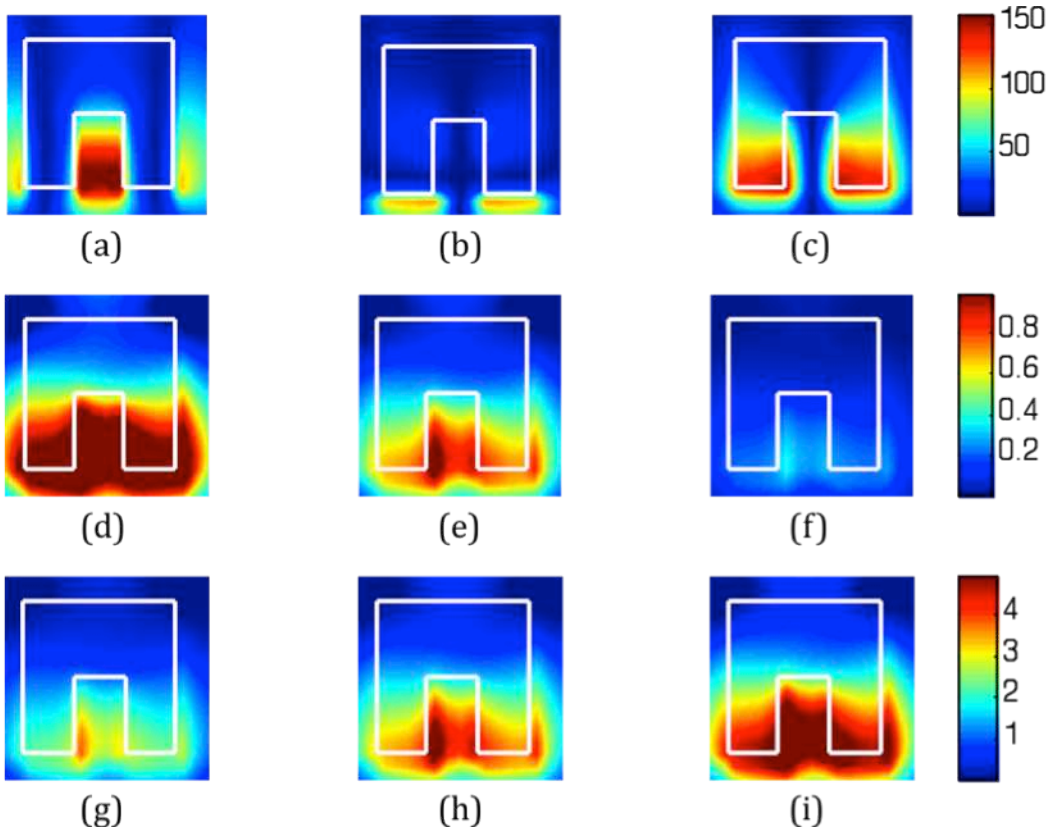

Figure S1: The first row corresponds to the electric field amplitude distributions at 175THz with pump ($P_0 = 3 \times 10^9\ s^{-1}$ and $\Delta t = 5ps$) in the cross-section of the gain layer (z = 40nm from the top of the structure) for different components: (a) E_x (V/m), (b) E_y (V/m), and (c) E_z (V/m). The second row corresponds to the near-field differential ΔE with $P_0 = 3 \times 10^9\ s^{-1}$ for three different time delays, namely (d) 5ps, (e) 45ps, and (f) 135ps, respectively. The third row corresponds to the near-field differential, ΔE at $\Delta t = 5ps$, for three different pumping strengths, namely (g) $P_0 = 6 \times 10^9\ s^{-1}$, (h) $P_0 = 9 \times 10^9\ s^{-1}$, and (i) $P_0 = 12 \times 10^9\ s^{-1}$, respectively. Here the ΔE is defined by taking the difference of the measured total electric field with pumping the active structure minus the same without pumping. The area enclosed by the white line is the projection of the SRRs on the gain layer.

This figure does not add significantly in understanding the mechanisms of optical changes of the gain medium: The spatial distribution of the gain is only marginally of interest to understand the effect of the pump on the differential transmission of the probe pulse. As we demonstrate in the paper, the major factors responsible for the experimentally observed behavior are the change in impedance of the metamaterial and the change of resonant absorption mediated by the SRR resonance, both with respect to the probe pulse. These two factors are global quantities that relate to the effective response of the metamaterial and have no "simple" correspondence to the local field distributions.

In Fig. S2 below we show a typical example of the spatial distribution of the population inversion, $\Delta N = N2\text{-}N1$, between the lasing levels which can serve as a measure for the spatial distribution of the gain in our samples. The cross-section plane of the plot is parallel to the surface in the middle of the gain layer underneath the SRR. As expected, the depletion of the population inversion follows the strength of the local E field and is strongest in the gap of the SRR. Note the very small scale of the depletion of population inversion; this indicates that this active metamaterial is working deep within the linear response regime and is far from gain saturation.

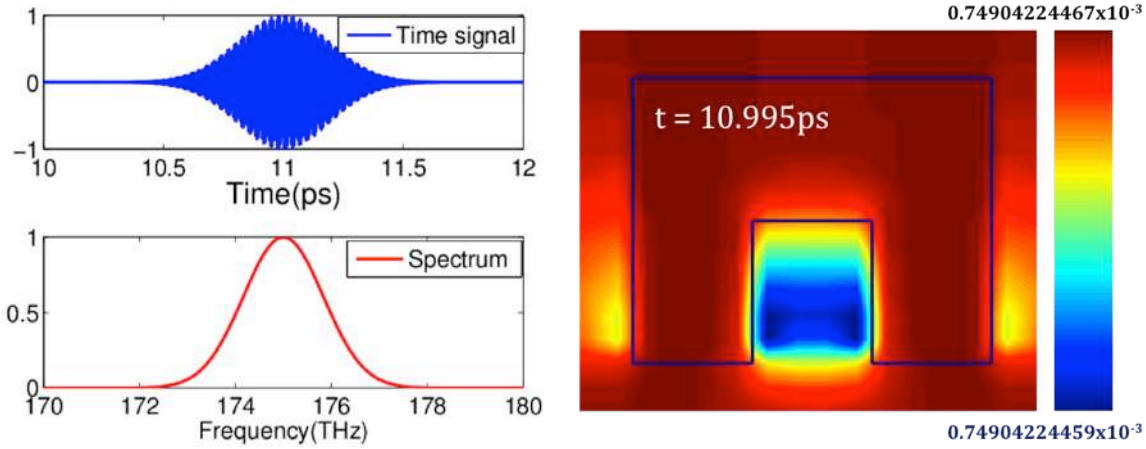

Figure S2: The normalized spatial distribution of population inversion $(N_2\text{-}N_1)/N_{total}$ is shown at absolute time t = 10.995ps in the right panel. The population inversion is plotted in the cross-section parallel to the surface in the middle of the gain layer. The pump pulse is centered around 6ps, the probe pulse at 11ps; the pump-probe delay is 5ps. The pumping rate is $3\text{x}10^9$ s^{-1}, and the center frequency and FWHM of probe pulse are 175THz and 2THz (see Fig. 2). The left panels show the shape of the transmitted probe pulse in time domain (top) and in frequency domain (bottom). Note that the depletion of the population inversion is very small; the pulse transmission takes place deep within the linear response regime.

We did not further investigate the pump-field spatial distribution, as this is essentially constant in our implementation via a Gaussian pumping rate. The fact we can demonstrate the negative differential transmissions and successfully attribute them to reflectance and absorptance changes brought about by the line width change in the metamaterial resonance proves that the spatial variation of the pump field is inconsequential and not responsible for the observed effect.

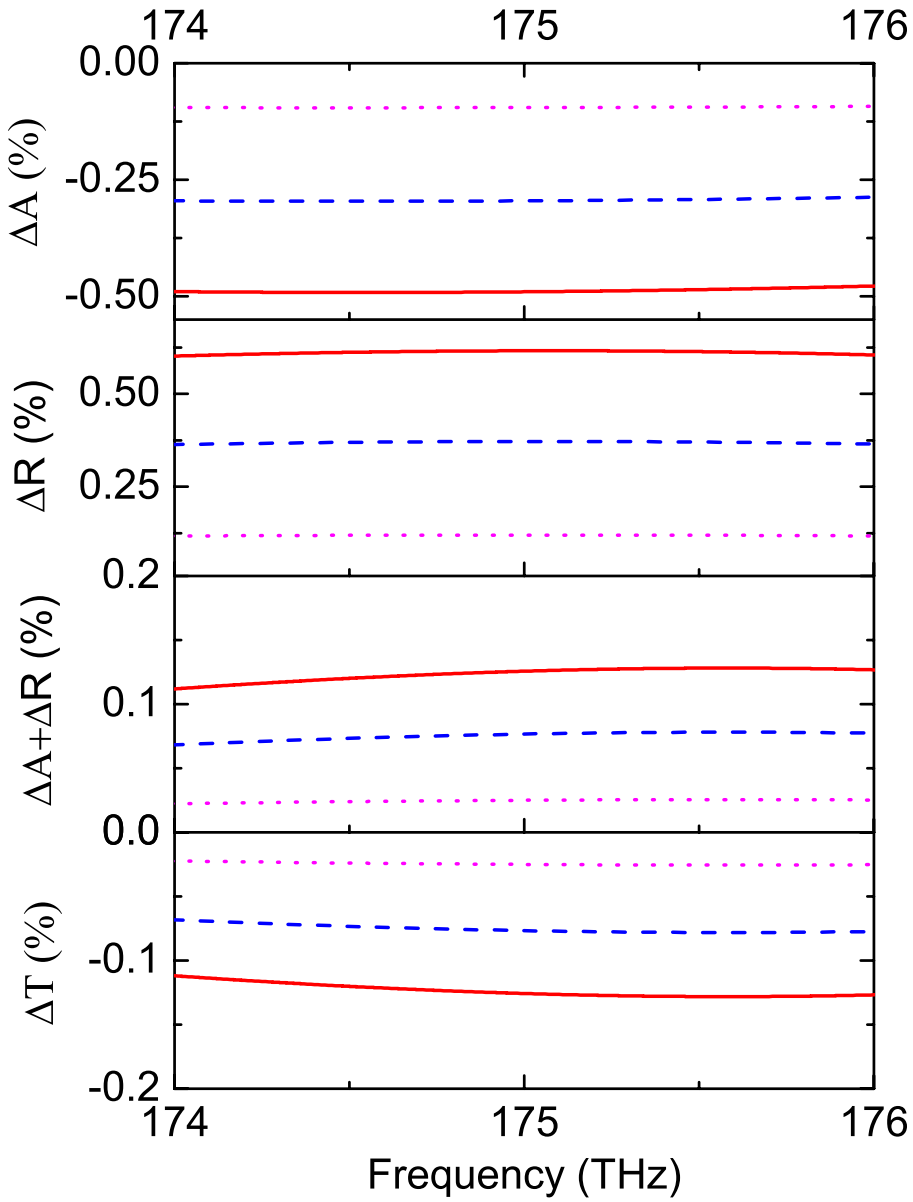

Figure S3: Frequency domain numerical pump-probe experiments results for the on-resonance case (see Fig. 5) for a pump-probe delay of 5ps (red solid curve), 45ps (blue dashed curve) and 135ps (magenta dotted curve), respectively. Here ΔT, ΔR and ΔA are the change in transmittance, reflectance and absorptance, respectively, between the pumped and unpumped case.

In Fig. S3 we present some additional results for the change in transmittance, reflectance, and absorptance between the pumped and unpumped cases augmenting Fig. 5 in the manuscript. We consistently observe a negative differential transmittance for probe pulses centered at the resonance frequency of the SRR (2THz probe pulse bandwidth, on-resonance case). We show the results for three different pump-probe delays ranging from 5ps to 135ps. The 5ps case (red solid line) corresponds to the case shown in Fig. 5. The differences between the curves shown in Fig. S3 result from the exponential decay of the

population inversion created by the pump (available gain) with increasing pump-probe delay due to non-radiative decay in the rate equations. Thus, the longer we wait, the smaller the effective gain. We see that the absorptance change, ΔA, becoming less negative, the reflectance change, ΔR, and the transmittance change, ΔT, becoming smaller with increasing pump-probe delay. All three cases maintain the negative differential transmittance. However, in all cases the increase in reflectance (due to increased impedance mismatch near the undamped resonance) is the dominant contribution to the differential transmittance, rendering it negative despite the negative sign in the differential absorptance. These results corroborate the analysis in the paper.

Finally, we want to take the opportunity to put our results in perspective with respect to the ongoing debate [cf. M. I. Stockman, PRL 106, 156802 (2011); S. Wuestner, A. Pusch, K. L. Tsakmakidis, J. M. Hamm, O. Hess, PRL 107, 259701 (2011); J. B. Pendry, S. A. Maier, PRL 107, 259703 (2011)] within the community as to whether complete compensation and net amplification in active metamaterials is possible. The question of whether net amplification, i.e. absolute transmittance larger than unity, is possible or not is not really relevant for the experimentally observed behavior that we explain in this manuscript because we are actually far from total compensation in these experiments. While the differential transmissions may be positive or negative, the absolute absorptance here remains positive. In our simulations, we do easily observe negative total absorptance and net amplification if we increase the pumping rate to experimentally unrealistic levels (here $P_o \approx 10^{11}\,s^{-1}$). This is in agreement with results demonstration loss compensation and over-compensation in numerical work we published before (see e.g. Ref. 4 in the manuscript). As is well known e.g. from laser devises, instability arises when the gain exceeds both intrinsic and radiation loss and lasing and saturation of gain ensues in this case. If, however, the gain just compensates the intrinsic absorption but not the radiation damping then stable amplification is possible. The same applies in metamaterials with gain at sufficiently high pumping rates. In real active metamaterials the situation may become more complicated. For near optical materials, all resonances arising from the metamaterial constituents are plasmonic in nature to some extent. Parallel to the normally desired radiative modes that lead to attenuation or amplification of transmitted signal radiation (and which will lase for high enough gain) also non-radiative modes exist (which may lead to spasing for high enough gain). The latter compete for the available gain and may prevent overcompensation or lasing if less damped intrinsically. In our simulations we have not observed that, but the simulations in the case of this manuscript are not designed to be accurate in the lasing limit because although including possible spasing solutions they do not handle the background fluctuations correctly (as they are inconsequential for the situation far below the lasing threshold which we are discussing in the manuscript). The overcompensation and amplification we observe at unrealistically high pumping rates may indicate that spasing does not outcompete the propagating modes for gain in our materials or may just be a consequence of the spasing modes not being excited by either the probe radiation or the background noise. Thus, deciding the question of whether lasing or spasing modes win the competition for the gain and whether lasing from metamaterials with gain is possible requires more careful simulations and is clearly beyond the scope and purpose of this manuscript.